Path Integral Analysis of random Lotka-Volterra ecosystems

University of Manchester

Semester 2 Report

Joshua Holmes
with Sebastian Castedo
Supervised by Tobias Galla

May 2023

Abstract

We make use of dynamical mean field theory to study the dynamics of Lotka-Volterra ecosystems with random interaction matrices. These matrices are generated with generalised correlations. The impacts of these correlations on the stability of the resulting ecosystem is studied analytically and then compared with simulation. The results suggest that two previously ignored correlations have a significant effect on the overall stability of the ecosystem therefore they should be considered in subsequent analyses and studied further.

Contents

1 Introduction

For many years, the Stability-Diversity debate has been at the forefront of ecology and it is still ongoing to this day[1]. The resolution to this argument appears to hold growing practical significance, given the apparent unprecedented decline in biodiversity observed in recent years [2, 3, 4, 5]. The impacts of climate change are expected to worsen this over the coming years [6, 7, 8, 9]. As a direct result of this, a theoretical understanding of the relationship between the structure of an ecosystem and its stability will be more important than ever. As large scale ecosystem surveys are costly, difficult to repeat, and often take years, a theoretical treatment compared with computer simulations could be very instructive.

Early research suggested that increased complexity would lead to more stable ecosystems [10, 11]. In particular, Charles Elton [10] contended that "simple communities were more easily upset than that of richer ones; that is, more subject to destructive oscillations in populations, and more vulnerable to invasions". This was challenged by Robert May's analysis [12, 13]. Building on the work of Ashby and Gardner [14], May used random matrix theory and linear stability analysis to find relationships between the connectance of community matrices and the stability of the resulting dynamics. The results of this implied that increased diversity actually led to a decrease in stability. May's analysis was model independent and did not consider any particular dynamics which implies it can be applied generally.

In this study, we explore ecological systems by applying methods derived from statistical physics. Specifically, we focus on Lotka-Volterra communities, where interaction matrices are randomized. Our approach diverges from May's methodology as we aim to examine the influence of a random community matrix within a specific model. To conduct a comprehensive theoretical analysis of these complex ecosystems, we employ techniques from statistical mechanics tailored for disordered systems.

To this end, we utilize the Martin-Siggia-Rose-De Dominicis-Peliti-Janssen method, which leverages path integrals to derive effective dynamics governing a representative species within the population [15, 16, 17, 18, 19]. Similar to previous studies [20, 21], we adopt this methodology. At the stationary point of the resulting effective process, providing it is stable, we can extract information about the bulk statistics of the disordered system. It is worth noting that our approach holds validity under the limit as $N \to \infty$, where N represents the number of species in the system.

The Lotka-Volterra model describes the time evolution of an ecosystem of N species, labelled by $i = 1, ..., N$. The dynamics of this system are given by N coupled differential equations of the form

$$\frac{dx_i(t)}{dt} = r_i x_i(t) \left(K_i + \sum_{j=1}^{N} \alpha_{ij} x_j(t) \right) \tag{1}$$

where x_i is the number density of species i, and r_i is the basic growth rate. K_i is the carrying capacity which governs the maximum population size that can be sustained for a species given the resources within a particular environment [22]. α_{ij} gives the element of the community matrix describing the effect of species j on species i. A negative value implies that species j

is detrimental towards species i while a positive value implies the opposite. For the sake of simplicity, we set $r_i = 1$ and $K_i = 1$.

The specific purpose of this paper is to add correlations into the interaction matrix, α_{ij}, and investigate the the consequences for the stability of the system. In the past, correlations between diagonally opposite elements, e.g. α_{ij} and α_{ji} have been studied but more general correlations have been neglected.

2 Method

2.1 The Community Matrix

As discussed in Section 1, the purpose of this investigation was to consider the implications of generalized correlations on the dynamics of a Lotka-Volterra ecosystem. To make the investigation as general as possible, we considered all possible pairwise correlations, these are as such:

$$\begin{aligned} \text{Var}(z_{ij}) &= \frac{\sigma^2}{N}, \\ \text{Corr}(z_{ij}, z_{ji}) &= \Gamma, \\ \text{Corr}(z_{ij}, z_{ki}) &= \frac{\gamma}{N}, \\ \text{Corr}(z_{ij}, z_{ik}) &= \frac{r}{N}, \\ \text{Corr}(z_{ji}, z_{ki}) &= \frac{c}{N}, \end{aligned} \tag{2}$$

similarly to [23]. In order to generate the required correlations, we decompose z_{ij} in the following way

$$z_{ij} = \beta_i + \kappa_j + \omega_{ij} \tag{3}$$

for all $i \neq j$. β_i, κ_j, and ω_{ij} are Gaussian zero-mean random variables. In order to generate the intended correlations in our interaction matrix, the following covariance matrices have to be satisfied:

$$\begin{aligned} \begin{pmatrix} \overline{\beta_i^2} & \overline{\beta_i \kappa_i} \\ \overline{\beta_i \kappa_i} & \overline{\kappa_i^2} \end{pmatrix} &= \frac{\sigma^2}{N^2} \begin{pmatrix} r & \gamma \\ \gamma & c \end{pmatrix} \\ \begin{pmatrix} \overline{\omega_{ij}^2} & \overline{\omega_{ij}\omega_{ji}} \\ \overline{\omega_{ij}\omega_{ji}} & \overline{\omega_{ji}^2} \end{pmatrix} &= \frac{\sigma^2}{N} \begin{pmatrix} 1 - \frac{(r+c)}{N} & \Gamma - \frac{2\gamma}{N} \\ \Gamma - \frac{2\gamma}{N} & 1 - \frac{(r+c)}{N} \end{pmatrix}. \end{aligned} \tag{4}$$

The non-diagonal elements of the matrix can then be generated using

$$\alpha_{ij} = \frac{\mu}{N} + \frac{\sigma}{\sqrt{N}} z_{ij} \tag{5}$$

with μ, σ, N being the mean value of the non-diagonal elements of the community matrix, the square root of the variance of interactions, and the number of species in the ecosystem respectively. The scaling of these equations by N is necessary so as to produce a well-defined thermodynamic limit as $N \to \infty$. The diagonal elements are set to -1 to ensure that the system will be stable in the absence of interactions. The matrices in 4 can be split and used to generate the z_{ij} elements using Cholesky decomposition[24, 25].

The community matrix can now be constructed with the required correlations. A physical interpretation of these correlations can be understood as follows: Γ gives the correlation between diagonally opposite values of the interaction matrix, when $\Gamma = -1$, elements z_{ij} will always have the opposite sign to element z_{ji}, leading to 100% of the interactions between species having predator-prey dynamics. In contrast, a value of $\Gamma = 1$ will result in the opposite behaviour, 0% predator-prey pairs.

The value of r is gives the correlation between elements within the same row. Physically, a high value of r implies that all species within the ecosystem will have a similar effect on species i. This is similar to c which gives the 'in-column' correlations within the system. A high value of c would result in an ecosystem in which, for example, species i would have a similar impact on all other species.

The value of γ gives the

2.2 Generating Functional Analysis

As stated in section 1, we used the Martin-Siggia-Rose-De Dominicis-Peliti-Janssen method to produce the effective dynamics for our system [15, 16, 17, 18, 19]. This closely follows a previous analysis performed by Galla [20]. In order to perform the generating functional analysis, we consider

$$\frac{dx_i(t)}{dt} = x_i(t)\left(1 + \sum_{j=1}^{N} \alpha_{ij} x_j(t) + h(t)\right) \tag{6}$$

which is Eq. (1) with an added perturbation field $h(t)$. This is a theoretical device which be used to generate dynamical response functions and set to zero at the end of the calculations.

The generating functional is defined as

$$Z[\psi] = \int D\mathbf{x}\delta(\text{equations of motion}) e^{i\sum_i \int dt x_i(t)\psi_i(t)}, \tag{7}$$

where δ is the Dirac delta distribution [26]. This ensures that the calculation is only performed over the paths specified by the equation of motion, which in this case is Eq. (6). Inserting the

relevant equations of motion into Eq. (7) gives

$$\begin{aligned} Z[\psi] = \int D\mathbf{x} \prod_{it} \exp\left(i \sum_i \int dt x_i(t)\psi_i(t) \right) \\ \times\delta\left(\frac{\dot{x}_i}{x_i} - \left[1 + \sum_{j=1}^{N} \alpha_{ij} x_j(t) + h(t) \right] \right), \end{aligned} \tag{8}$$

where Eq. (6) has been divided on both sides by x_i beforehand to simplify the calculations and $\dot{x} = \frac{dx}{dt}$. The Dirac delta function can be represented as a Fourier transform [27], with the form

$$\delta(x - \alpha) = \int_{-\infty}^{\infty} e^{i(x-\alpha)k} Dk, \tag{9}$$

Where $Dk = \frac{dk}{2\pi}$. We can convert the delta functions from Eq. (8) into this form to give

$$\begin{aligned} Z[\psi] = \int D\mathbf{x} D\hat{\mathbf{x}} \exp\left(i \sum_i \int dt x_i(t)\psi_i(t) \right) \\ \times\exp\left(i \sum_i \int dt \left[\hat{x}_i \left\{ \frac{\dot{x}_i}{x_i} - [1 + \sum_{j=1}^{N} \alpha_{ij} x_j(t) + h(t)] \right\} \right] \right), \end{aligned} \tag{10}$$

where $\hat{x}$ denotes the conjugate variable for the Fourier transform.

2.3 Carrying out Disorder Average

The next step is to perform a Gaussian average over the terms contributing to the disorder of the system. In the case we are considering, the disorder is entirely contained within the α_{ij} term which is defined for $i < j$ in Eq. (5). The term within the generating functional which contains the disorder is

$$X \equiv \exp\left(-i \sum_{i \neq j} \int dt \hat{x}_i(t) \alpha_{ij} x_j(t) \right), \tag{11}$$

we would like to average over the disorder in this term. To start, we separate α_{ij} using Eqs. (5) and (3) and then perform an average which gives

$$\begin{aligned} \overline{X} &= \overline{\exp\left(-i \sum_{i \neq j} \int dt \hat{x}_i(t) \alpha_{ij} x_j(t) \right)} \\ &= \exp\left(-i \frac{\mu}{N} \sum_{i \neq j} \int dt \hat{x}_i(t) x_j(t) \right) \times \overline{\exp\left(-i \frac{\sigma}{\sqrt{N}} \sum_{i \neq j} \int dt \hat{x}_i(t) z_{ij} x_j(t) \right)}. \end{aligned} \tag{12}$$

As the first factor contains no disorder, we consider only the second term for now. We define this as

$$Y \equiv \exp\left(-i\frac{\sigma}{\sqrt{N}}\sum_{i\neq j}\int dt\hat{x}_i(t)z_{ij}x_j(t)\right), \tag{13}$$

which can also be written as

$$Y = \prod_{i<j}\exp\left(-i\frac{\sigma}{\sqrt{N}}\int dt[\hat{x}_i(t)z_{ij}x_j(t)+\hat{x}_j(t)z_{ji}x_i(t)]\right). \tag{14}$$

Each pair $i<j$ gives a factor Y_{ij} defined by

$$Y_{ij} \equiv \exp\left(-i\frac{\sigma}{\sqrt{N}}\sum_{i\neq j}\int dt\,[\hat{x}_i(t)(\beta_i+\kappa_j+\omega_{ij})x_j(t)+\hat{x}_j(t)(\beta_j+\kappa_i+\omega_{ji})x_i(t)]\right). \tag{15}$$

2.4 Introducing Order Parameters

To make the algebra manageable, we introduce some macroscopic order parameters as shorthands:

$$\begin{aligned}
M(t) &= \frac{1}{N}\sum_i x_i(t),\\
P(t) &= i\frac{1}{N}\sum_i \hat{x}_i(t),\\
C(t,t') &= \frac{1}{N}\sum_i x_i(t)x_i(t'),\\
K(t,t') &= \frac{1}{N}\sum_i x_i(t)\hat{x}_i(t'),\\
L(t,t') &= \frac{1}{N}\sum_i \hat{x}_i(t)\hat{x}_i(t').
\end{aligned} \tag{16}$$

These should simplify things as we move forward. Following the Gaussian integration [28] and implementation of the parameters in Eqn. (16) we find:

$$\begin{aligned}
\overline{X} = \exp\Big[-\mu N\int dtP(t)M(t) - \frac{1}{2}N\sigma^2\int dt\int dt' rL(t,t')M(t)M(t') - cC(t,t')P(t)P(t')\\
- 2\gamma iK(t,t')M(t)P(t') + L(t,t')C(t,t') + \Gamma K(t,t')K(t',t) + \mathcal{O}(N^0)\Big]
\end{aligned} \tag{17}$$

where $\mathcal{O}(N^0)$ indicates that sub-leading contributions in N have been removed. This is because we will eventually take the limit $N\to\infty$ so these terms will not contribute to the final result

and can be neglected. We then can introduce these parameters into the generating functional as delta-functions in their integral representations. The disorder-averaged generating functional can be written in terms of the order parameters as follows

$$\overline{Z}[\underline{\psi}] = \int D[\underline{M}, \underline{\underline{C}}, \underline{\underline{L}}, \underline{\underline{K}}, \underline{P}, \underline{\hat{M}}, \underline{\underline{\hat{C}}}, \underline{\underline{\hat{L}}}, \underline{\underline{\hat{K}}}, \underline{\hat{P}}] \cdot e^{\left(N\left[\Psi+\Phi+\Omega+\mathcal{O}(N^{-1})\right]\right)}. \tag{18}$$

Where the terms with the hats represent the conjugate of the respective order parameter which has been chosen such that the exponent contains the pre-factor N. The term

$$\begin{aligned}\Psi = & i \int dt[\hat{M}(t)M(t) + \hat{P}(t)P(t)] \\ & + i \int dtdt' \left[\hat{C}(t,t')C(t,t') + \hat{K}(t,t')K(t,t') + \hat{L}(t,t')L(t,t')\right]\end{aligned} \tag{19}$$

results from the introduction of the order parameters whilst the contribution

$$\begin{aligned}\Phi = & -\frac{1}{2}\sigma^2 \int dt \int dt' \Big[L(t,t')C(t,t') + \Gamma K(t,t')K(t',t) + rL(t,t')M(t)M(t') \\ & - cC(t,t')P(t)P(t') - 2\gamma i K(t,t')M(t)P(t')\Big] \\ & - \mu \int dt M(t)P(t)\end{aligned} \tag{20}$$

comes from the disorder average, and Ω describes the details of the microscopic time evolution

$$\begin{aligned}\Omega = & N^{-1} \sum_i \log \Bigg[\int D[x_i, \hat{x}_i] p_0^i(x_i(0)) \exp\left(i \int dt \psi_i(t) x_i(t)\right) \\ & \times \exp\left(-i \int dtdt' \left[\hat{C}(t,t')x_i(t)x_i(t') + \hat{L}(t,t')x_i(t)x_i(t') + \hat{K}(t,t')x_i(t)x_i(t')\right]\right) \\ & \times \exp\left(i \int dt \hat{x}_i(t) \left(\frac{\dot{x}_i(t)}{x_i(t)} - [1 - x(t)] - h(t)\right)\right) \\ & \times \exp\left(-i \int dt[\hat{M}(t)x_i(t) + \hat{P}(t) i \hat{x}_i(t)]\right).\end{aligned} \tag{21}$$

The quantity p_0^i describes the distribution from which the initial values of $\{x_i\}$ are drawn.

2.5 Saddle-point Analysis

We use the saddle-point method [29, 30] to evaluate Eqn. (18). We do this by extremising the generating functional with respect to the order parameters and then following through with the integration. In the process of this, we introduce a response function:

$$G(t,t') = \left\langle \frac{\delta x(t)}{\delta h(t')} \right\rangle_*. \tag{22}$$

This method gives the following generating functional for the effective process:

$$\begin{aligned} Z_{eff} = &\int D[x,\hat{x}]p_0(x(0))\text{exp}\left(i\int dt\hat{x}(t)\left(\frac{\dot{x}(t)}{x(t)} - [1-x(t)] - h(t) - \mu M(t)\right)\right) \\ &\times \exp\left(-\sigma^2\int dt\int dt'\left[\frac{1}{2}\hat{x}(t)\hat{x}(t')(rM(t)M(t') + C(t,t'))\right.\right. \\ &\left.\left. + iG(t,t')[\Gamma x(t)\hat{x}(t') + \gamma\hat{x}(t)M(t)]\right]\right). \end{aligned} \tag{23}$$

From this, we obtain the effective dynamics for the process:

$$\begin{aligned} \dot{x}(t) = x(t)\Bigg[1 - x(t) + \Gamma\sigma^2\int dt'G(t,t')x(t') \\ + \gamma\sigma^2\int dt'G(t,t')M(t') + \mu M(t) + \eta(t) + h(t)\Bigg] \end{aligned} \tag{24}$$

where

$$\langle\eta(t)\eta(t')\rangle_* = \sigma^2\Big(\langle x(t)x(t')\rangle_* + rM(t)M(t')\Big) \tag{25}$$

and where $\langle ...\rangle_*$ denoted an average over realizations of the effective dynamics (24). This is to be evaluated at $h = 0$.

2.6 Fixed Point Analysis

Now that the effective process has been found, we assume the existence of fixed points and look to evaluate it at the limit as where $x(t)|_{t\to\infty} = x^*$. From this, we can see that the fixed point equations can be found by solving

$$x^*\left[1 - x^* + \Gamma x^*\sigma^2\int_0^\infty G(\tau)d\tau + \gamma\int d\tau G(\tau)M^* + \mu M^* + \eta^*\right] = 0 \tag{26}$$

where $G(t,t')$ has been rewritten as $G(\tau)$ as it is a function of time differences only. The solutions of this equation then allow us to extract the bulk statistics of the system through a set of closed integral equations:

$$\begin{aligned} \phi &= \int_{-\infty}^{\Delta} Dz, \\ M^* &= \sigma\frac{\sqrt{q + rM^{*2}}}{1 - \Gamma\sigma^2\chi}\int_{-\infty}^{\Delta} Dz(\Delta - z), \\ q &= \sigma^2\frac{q + rM^{*2}}{(1 - \Gamma\sigma^2\chi)^2}\int_{-\infty}^{\Delta} Dz(\Delta - z)^2, \\ \chi &= \frac{1}{1 - \Gamma\sigma^2\chi}\int_{-\infty}^{\Delta} Dz, \end{aligned} \tag{27}$$

where

$$\Delta = 1 + \frac{M^*[\mu + \gamma\sigma^2\chi]}{\sigma\sqrt{q + rM^{*2}}}. \tag{28}$$

We define

$$w_l(\Delta) \equiv \int_{-\infty}^{\Delta} Dz(\Delta - z)^l. \tag{29}$$

2.7 Solution Procedure

These In order to generate the required relations, we can fix the values of μ, and γ to obtain $\sigma^2, q, \chi,$ and M as functions of Δ.

Through algebraic manipulation of the relations in equations (27) and (28), we finally come upon the relations

$$\begin{aligned}
\chi &= w_0 + \frac{w_0^2}{w_2}\frac{\Gamma}{1 + r\frac{w_1^2}{w_2}}, \\
\sigma^2 &= \frac{w_2}{\left[w_2 + \frac{\Gamma w_0}{1+\frac{rw_1^2}{w_2}}\right]^2\left(1 + \frac{rw_1^2}{w_2}\right)}, \\
\frac{1}{M} &= \frac{\Delta w_2\left(1 + \frac{rw_1^2}{w_2}\right) - \gamma w_0 w_1}{w_1\left[w_0\Gamma + w_2\left(1 + \frac{rw_1^2}{w_2}\right)\right]} - \mu, \\
q &= \frac{M^2 w_1^2}{w_2}, \\
\phi &= w_0.
\end{aligned} \tag{30}$$

This allows us to calculate M, q, ϕ as a function of σ^2 in parametric form.

The physical interpretations of the parameters in equations (30) are as follows:

- The quantity $\phi = w_0$ is the fraction of surviving species once the system reaches stability.
- The quantity M is the mean abundance per species, $M = \frac{1}{N}\sum_{i=1}^{N} x_i^*$. This can also be thought of as the first moment of the abundances.
- The quantity q is $q = \frac{1}{N}\sum_{i=1}^{N}(x_i^*)^2$ or the second moment of the abundances.
- The quantity χ is a susceptibility which measures how strongly species abundances change as a result of an external perturbation.

2.8 Stability Analysis

Our analysis can also reveal the conditions in which the system in question does not have a unique, stable fixed point. There are two causes of this: (1) Linear instability of the fixed point solutions, or (2) the average abundance, M can diverge.

We first consider linear instability, and perform a stability analysis of the solutions along the lines of [21, 20]. We add white noise $\epsilon\xi(t)$ to the effective process where ξ is a Gaussian white noise term which has a mean of 0 and unit variance. We then study fluctuations $\epsilon y(t)$ about a fixed point of Eqn. (24) and write

$$x(t) = x^* + \epsilon y(t) \tag{31}$$

and denote the additional term by $\epsilon v(t)$. We linearise in ϵ. For the case $x^* = 0$. We then study the fluctuations about a fixed point:

$$\frac{dy(t)}{dt} = x^* \left[-y(t) + \Gamma\sigma^2 \int_0^t G(t,t')y(t')dt' + v(t) + \xi(t) \right]. \tag{32}$$

We then consider the non-zero fixed point and convert to Fourier space. We then obtain

$$\langle |\tilde{y}(0)|^2 \rangle = \frac{\phi(\sigma^2 r M^2 + 1)}{[\Gamma\sigma^2\chi - 1]^2 - \phi\sigma^2} \tag{33}$$

which indicates that $\langle |\tilde{y}(0)|^2 \rangle$ diverges when $\phi\sigma^2 = (1-\Gamma\sigma^2\chi)^2$. One finds $\phi\sigma^2 < (1-\Gamma\sigma^2\chi)^2$ in the stable phase. We find that this corresponds to $\phi = \frac{1}{2}$ and we can simplify this stability relation to the following:

$$\sigma_c^2(\Gamma) = \frac{2}{(1+\Gamma)^2}. \tag{34}$$

It is worth highlighting that the linear stability of the ecosystem is determined solely by two factors: σ^2 and Γ, where σ^2 is a function of both Γ and r. Consequently, out of the four correlations examined, only the cross-correlations and the in-row correlations are expected to influence the linear stability.

Divergences in the ecosystem can be studied by taking the limit as the average abundance, M, approaches ∞. This gives us the relations

$$\begin{aligned} \sigma^2 &= \frac{w_2(1+\frac{rw_1^2}{w_2})}{\left[w_2(1+\frac{rw_1^2}{w_2}) + \Gamma w_0\right]^2}, \\ \mu &= \frac{\Delta w_2 \left(1+\frac{rw_1^2}{w_2}\right) - \gamma w_0 w_1}{w_1 \left[w_0\Gamma + w_2\left(1+\frac{rw_1^2}{w_2}\right)\right]}, \end{aligned} \tag{35}$$

which can be solved parametrically to give the line of stability. While this is harder to analyse by inspection compared to the linear instability case, we can infer that $\Gamma, r,$ andγ should all have an impact on the occurrence of divergences.

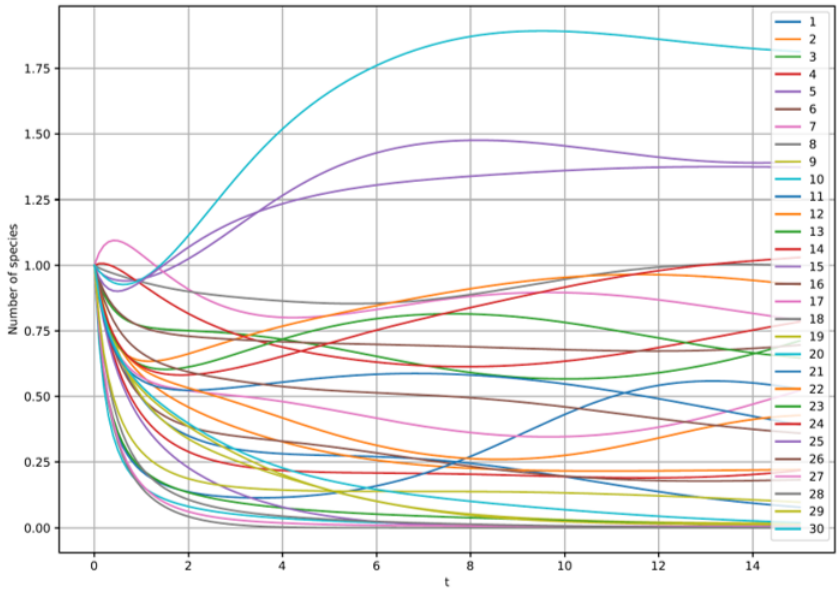

Figure 1: This graphs show the variation of species abundance over time for one run of the simulation. For this example, the initial abundance was set to 1 for all species but in other simulations, the initial abundances were drawn from a Gaussian distribution. This example also only uses 30 species whilst our working simulations used between 300 and 400.

3 Results

3.1 Simulation

Following the analytical treatment given in Section 2, we compared the predictions to simulated data. In order to do this we generated random matrices with N species and the required correlations, using the specifications from Eqns. (2,3,4,5). We then ran the system using the dynamics from Eqn. (1) using a variation of the Runge-Kutta-Fehlberg method with dynamic time-stepping [31, 32, 33, 34]. An example trajectory plot is given in Fig. 1 showing the relative abundances of a number of species throughout the course of a run.

3.2 Predator-prey interactions

The first of the correlations we look at is Γ. This governs the correlation between diagonally opposite elements within the interaction matrix, i.e. α_{ij}andα_{ji}. This corresponds to the fraction of predator-prey pairs within an ecosystem with $\Gamma = 1$ leading to 0% predator-prey, $\Gamma = 0$ leading to 50% predator-prey and $\Gamma = -1$ leading to 100% predator-prey behaviour. Fig. 2 displays a stability phase diagram for varied values of Γ using Eqns. (34) and (35) to plot the dashed linear instability line and the solid $M \to \infty$ line. This gives similar behaviour to that found in [35].

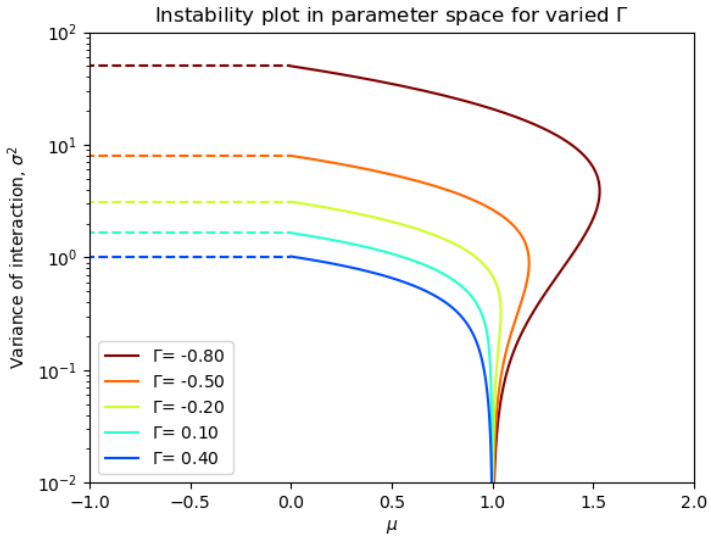

Figure 2: This plot shows a stability phase diagram for varied values of Γ. The dashed line represents the transition to linear instability and the solid line indicates the $M \to \infty$ transition. The area underneath and to the left of the curve is the stable region. It can be seen that lower values of Γ correspond to greater stability.

3.3 In-row Correlations

The second set of correlations to consider are the in-row correlations, represented by r. They are the correlations between all the elements in each respective row of the interaction matrix i.e. α_{ij}andα_{ik}. Physically they would refer to the correlations found between how all other species in the ecosystem impact species i. Fig. 3 demonstrates the impact of varying r. The average abundance of species within the system clearly increases with increased r, but the fraction of surviving species decreases. The simulation data strongly supports these conclusions, increasing the faith in our analysis.

We now turn to the effects that the in-row correlations have on the stability of an ecosystem, Fig. 4 shows a phase diagram of the stable region for varied r. It should be noted that an increase in r changes the stability system in a complex way, i.e. it has an opposite effect on the two forms of instability. The system is made more stable with regards to the transition to linear instability, but less stable with regards to possible divergences.

This seems like an unusual result. In order to empirically test this outcome, we ran a number of simulations with varied values of σ to test whether instabilities would appear at the points predicted by Fig. 4. The two types of instabilities need to be tested in different ways as they manifest differently. Past the linear instability transition, the system can still find a fixed point, it is just no longer stable, while past the $M \to \infty$ transition, the system will diverge. Therefore, to find the $M \to \infty$ transition point, we run many simulations with varied σ^2 for fixed values

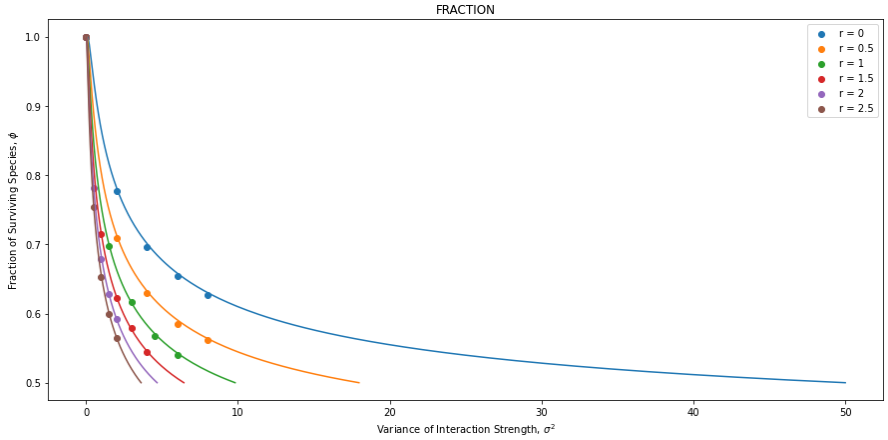

(a)

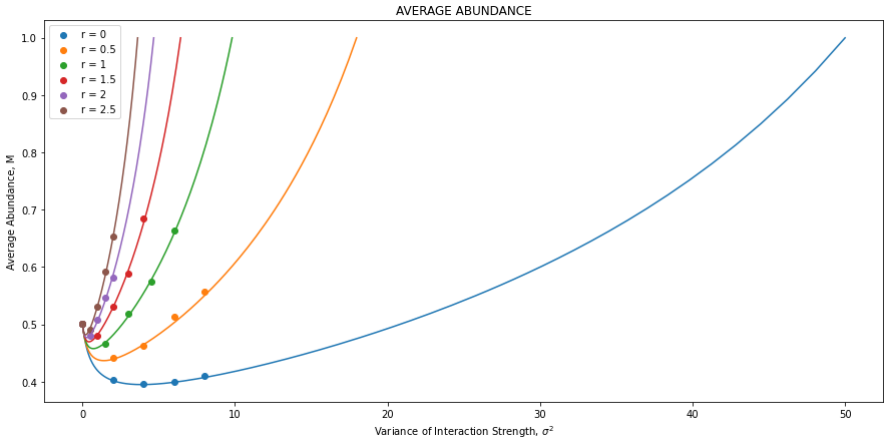

(b)

Figure 3: a) This plot shows the variation of the fraction of surviving species at the end of the simulation against σ^2. This was done for six values of the interaction coefficient r. b) This plot shows the variation of the average biomass at the end of the simulation against σ^2. This was also done for six values of r. Each data point in both of these plots were generated by simulating a 300 species ecosystem and averaging this over 20 iterations. They were done with r values of 0, 0.5, 1.0, 1.5, 2.0, and 2.5 respectively. The results of the simulation are compared to the theory line based on Eqn. (30). For these particular plots, $\Gamma = -0.8, \gamma = 0, c = 0$. The theory lines end at the onset of instability.

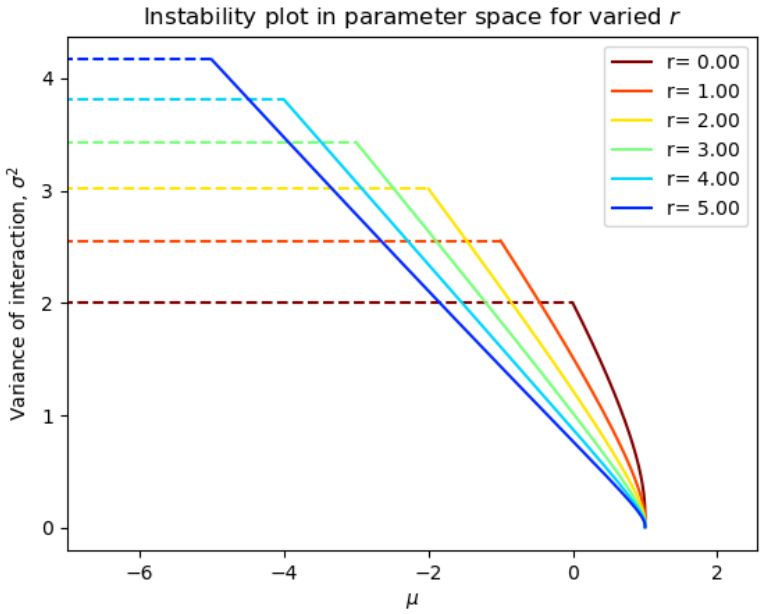

Figure 4: This plot shows a stability phase diagram for varied values of r. The dashed line represents the transition to linear instability and the solid line indicates the $M \to \infty$ transition. The area underneath and to the left of the curve is the stable region. It can be seen that an increase in r leads to a greater degree of stability with respect to the transition to linear instability, less stability with regard to the $M \to \infty$ transition.

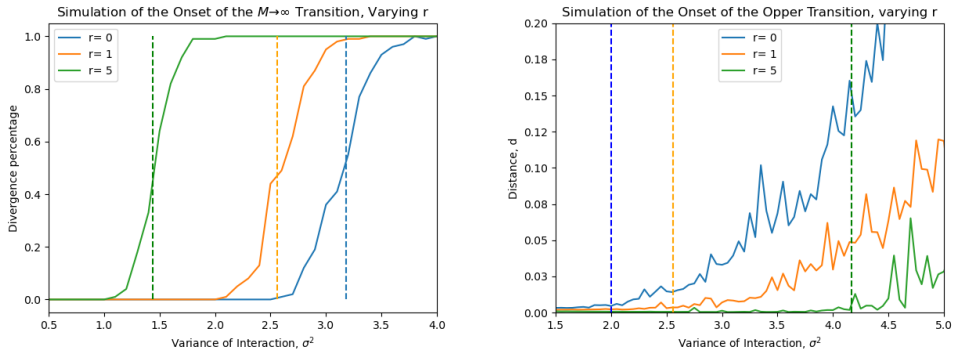

(a) (b)

Figure 5: a) This plot attempts to test where the $M \to \infty$ transition happens for three ecosystems with different values of r. To do this, μ and r are fixed and σ^2 is varied. Many simulations are performed for each data point and the fraction that diverge are measured. The vertical dashed line represents the theoretical prediction for the onset of instability. b) This plot measures the distance, d, which is the difference between values of x_i found at the end of the simulation. If a stable fixed point is reached, this value should be 0. The vertical dashed lines show the theoretical predictions for the onset of instability.

of μ and measure the fraction of divergent ecosystems at each step. For the transition to linear instability, we find the differences between the abundances at the end of different respective simulations. If the system reaches a unique, stable fixed point, this value should equal 0.

Fig. 5 shows that both the $M \to \infty$ and linear instability transitions happen at the predicted points, supporting the implications of Fig. 4.

3.4 In-column Correlations

The third type of correlations to consider are the in-column correlations, represented by c. Each column of the interaction matrix tells you how a single species affects all of the other species' within the ecosystem, so a high value of c would indicate that each species has a consistent impact across the ecosystem.

Interestingly, c does not make an appearance in the effective process, the parametrised equations or either of the stability equations. This implies that it has no effect of the bulk dynamics of the system. This is supported by Fig. 6 which shows that for both the fraction of surviving species, and the biomass, there is no difference between the varied values of c either in the theoretical predictions or the results of simulations.

As the value of c has no impact on any of the hyperparameters, it is trivial to note that it will also have no impact on either form of instability.

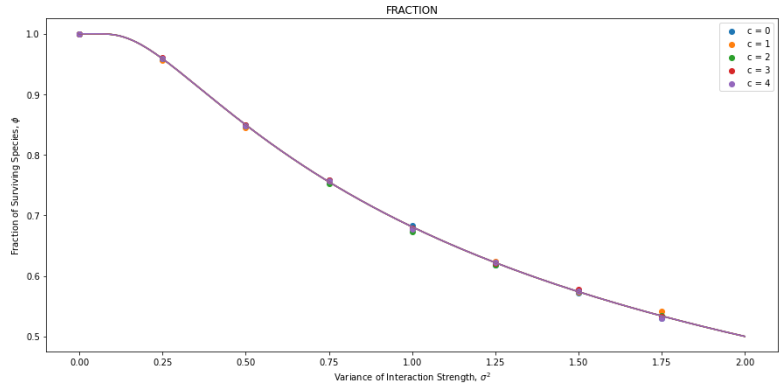

(a)

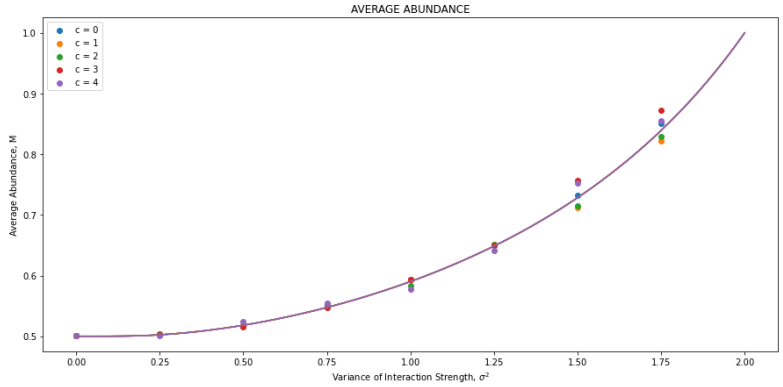

(b)

Figure 6: a) This plot shows the variation of the fraction of surviving species at the end of the simulation against σ^2. This was done for six values of the interaction coefficient c. b) This plot shows the variation of the average biomass at the end of the simulation against σ^2. This was also done for six values of r. Each data point in both of these plots were generated by simulating a 300 species ecosystem and averaging this over 20 iterations. They were done with c values of 0, 1, 2, 3, and 4 respectively. The results of the simulation are compared to the theory line based on Eqn. (30). For these particular plots, $\Gamma = -0.8, \gamma = 0, c = 0$. The theory lines end at the onset of instability.

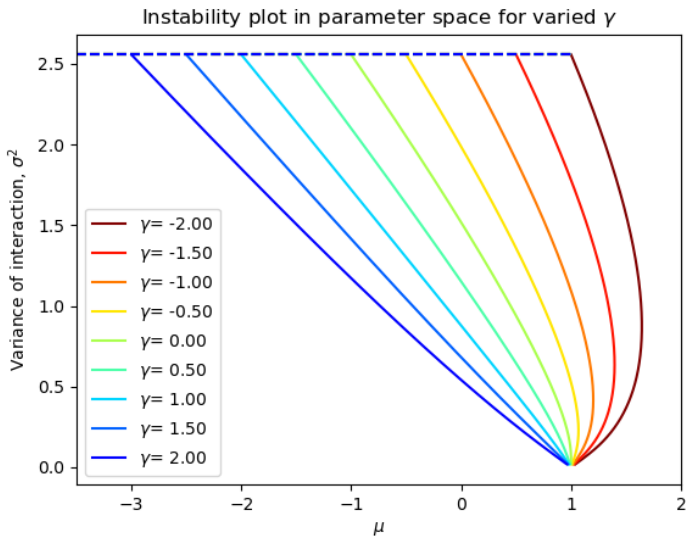

Figure 7: This plot shows a stability phase diagram for varied values of γ. The dashed line represents the transition to linear instability and the solid line indicates the $M \to \infty$ transition. The area underneath and to the left of the curve is the stable region. It can be seen that higher values of γ makes the system more likely to diverge but has no impact on the transition to linear instability.

3.5 Correlation between elements sharing an outside index

The final correlation to consider is γ, the correlation between elements sharing one index, i.e. α_{ij}andα_{ki}. This is the hardest of the correlations to visualise and has a more subtle effect on the matrix.

As predicted by Eqns. (34) and (35), and depicted in Fig. 7, γ has no impact whatsoever on the linear instability transition. It has a destabilising effect on the $M \to \infty$ transition.

This is supported empirically by the graphs in Fig. 8

This result can be explained by the fact that as shown in Eqn. (30), the fraction of surviving species, ϕ, is independent of the value of γ. The linear instability transition occurs in systems where the fraction of surviving species at the fixed point is less than $\frac{1}{2}$ at the fixed point, so a variable that does not affect ϕ will have no effect on the linear instability transition either.

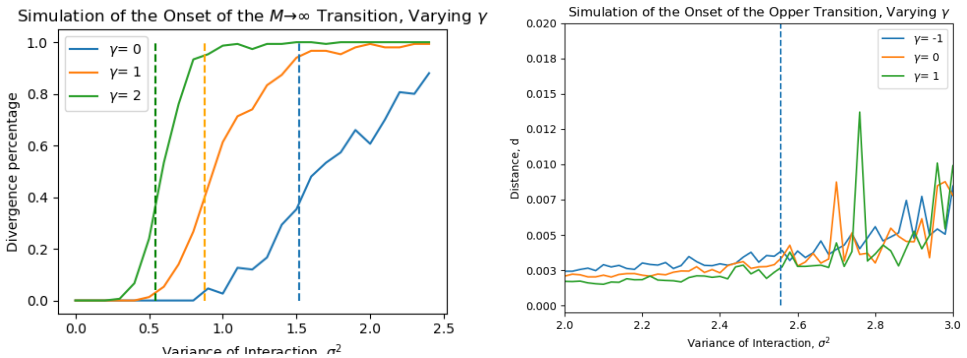

(a) (b)

Figure 8: a) This plot attempts to test where the $M \to \infty$ transition happens for three ecosystems with different values of γ. To do this, μ and γ are fixed and σ^2 is varied. Many simulations are performed for each data point and the fraction that diverge are measured. The vertical dashed line represents the theoretical prediction for the onset of instability. b) This plot measures the distance, d, which is the difference between values of x_i found at the end of the simulation. If a stable fixed point is reached, this value should be 0. The vertical dashed lines show the theoretical predictions for the onset of instability. It should be noted that the three values of γ all reach instability at the (same) predicted point.

4 Discussion

Following from the initial work done by May [12, 13], we have asked the same question but considered the potential dynamics of the system using the Lotka-Volterra model and applied generalised correlations to our random matrix. We then used dynamical mean field theory to analyse these equations and derive an effective process from which we extracted the bulk statistics of the system.

Other such analyses have taken place before [20], however correlations other than Γ have typically been neglected. Our work indicates that these correlations, specifically γ and r, cannot be ignored if the stability of the system is to be rigourously assessed. This is particularly relevant given the spontaneous emergence of correlations in initially uncorrelated systems after reaching a fixed point, resulting in species extinction [23, 36, 35].

It is clear from the results displayed that the correlation coefficients, other than c, have a significant impact on the stability of ecosystems at fixed points, via their effect on the hyperparameters of the system, namely ϕ and M. specifically, a large fraction of surviving species leads to a more stable system, as does an average abundance that has not seen a large increase. This implies that systems with a large number of species, each with a moderate population are more stable. This appears to match the empirical data [1].

It should be noted that measuring correlation coefficients in an ecosystem can be challenging due to various reasons. Further investigations can explore the direct impact of correlation

coefficients on the stability of ecosystems and the potential implications of our findings on ecological management and conservation efforts.

References

[1] McCann K. "The diversity-stability debate". In: *Nature* 405 (2000), pp. 428–233.

[2] Levin S. *Fragile Dominion: Complexity and the Commons*. Helix books, Reading, MA, 1999.

[3] Rasmussen J.B. Riciardi A. "Extinction Rates of North American freshwater fauna". In: *Conserv. Biol.* 13 (2000), pp. 1220–1222.

[4] Reid W.V. "Strategies for conserving biodiversity". In: *Environment* 39 (1997), pp. 16–43.

[5] Gergana N. Daskalova, Albert B. Phillimore, and Isla H. Myers-Smith. "Accounting for year effects and sampling error in temporal analyses of invertebrate population and biodiversity change: a comment on Seibold et al. 2019". In: *Insect Conservation and Diversity* 14 (2021).

[6] Sangita P. Ingole and Aruna U. Kakde. "Global Warming and Climate Change: Impact on Biodiversity". In: *International journal of scientific research* 2 (2012), pp. 381–384.

[7] Sadguru Prakash and Seema Srivastava. "Impact of Climate Change on Biodiversity: An Overview". In: *International Journal of Biological Innovations* (2019).

[8] Tan S. H. Habibullah M. S. Din B. H. "Impact of climate change on biodiversity loss: global evidence". In: *Environmental science and pollution research international* 29 (2022).

[9] Dejene W. Sintayehu. "Impact of climate change on biodiversity and associated key ecosystem services in Africa: a systematic review". In: *Ecosystem Health and Sustainability* 4 (2018), pp. 225–239.

[10] Elton C.S. *Ecology of Invasions by Animals and Plants*. Chapman & Hall, London, 1958.

[11] Macarthur R.H. "Fluctuations of animal populations and a measure of community stability". In: *Ecology* 36 (1955), pp. 533–536.

[12] May R.M. "Will a Large Complex System be Stable?" In: *Nature* 238 (1972), pp. 413–414.

[13] May R.M. *Stability and Complexity in Model Ecosystems*. Princeton Univ. Press, 1973.

[14] Ashby W.R. Gardner M.R. "Connectance of large dynamic (cybernetic) systems: critical values for stability". In: *Nature* 228 (1970), p. 784.

[15] De Dominicis C. In: *Phys. Rev. B* 18 (1978), p. 4913.

[16] Siggia E.D. Martin P.C. and Rose H.A. In: *Phys. Rev. A* 8 (1973), p. 423.

[17] Parisi G. Mezard M. and Virasoro M.A. *Spin Glass Theory and Beyond*. World Scientific Publishing - Singapore, 1993.

[18] Moss F. Coolen A.C. and Gielen S. "Statistical Mechanics of Recurrent Neural Networks II: Dynamics, in Handbook of Biological Physics". In: *Elsevier Science* 4 (2001), pp. 597–662.

[19] Kühn R. Coolen A.C. and Sollich P. *Theory of Neural Information Processing Systems*. Oxford University Press, Oxford, 2005.

[20] Galla T. "Dynamically evolved community size and stability of random Lotka-Volterra ecosystems". In: *EPL* 123 (48004), p. 1616.

[21] Diederich S. Opper M. "Phase transition and 1/f noise in a game dynamical model". In: *Phys. Rev. Lett.* 69 (1992), p. 1616.

[22] Byron C.J. Chapman E.J. "The flexible application of carrying capacity in ecology". In: *Global Ecology and Conservation* 13 (2018), e00365.

[23] Joseph W. Baron et al. "Eigenvalues of Random Matrices with Generalized Correlations: A Path Integral Approach". In: *PHYSICAL REVIEW LETTERS* 128.12 (2022), p. 120601.

[24] Johnson C.R. Horn R.A. *Matrix Analysis*. Cambridge University Press - Cambridge, 1985.

[25] Van Loan C. Golub G. *Matrix Computations*. John Hopkins - Baltimore, 1996.

[26] Dirac P. *The Principles of Quantum Mechanics*. Oxford University Press, 1930.

[27] Bracewell R. *The Fourier Transform and its Applications*. McGraw-Hill, 1984.

[28] Papoulis A. *Probability, Random Variables, and Stochastic Processes*. McGraw-Hill, 1984.

[29] Laplace P.S. "Mémoires de Mathématique et de Physique, Tome Sixième [Memoir on the probability of causes of events.]" In: *Statistical Science* 1 (1774), pp. 366–367.

[30] Butler R.W. *Saddlepoint approximations and applications*. Cambridge University Press, 2007.

[31] C.D.T. Runge. "Über die numerische Auflösung von Differentialgleichungen". In: *Mathematische Annalen, Springer* 46 (1895), pp. 167–178.

[32] Kutta M. "Beitrag zur näherungsweisen Integration totaler Differentialgleichungen". In: *Zeitschrift für Mathematik und Physik* 46 (1901), pp. 435–453.

[33] Moler C.B. Forsythe G.E. Malcolm M.A. *Computer Methods for Mathematical Computations,* Prentice-Hall, 1977.

[34] Shatalov M.Y. Adeniji A. Fadugba S. "Comparative analysis of Lotka-Volterra type models with numerical methods using residuals in Mathematica". In: *Communications in Mathematical Biology and Neuroscience* 2022 (2022).

[35] Joseph W. Baron et al. "Breakdown of Random-Matrix Universality in Persistent Lotka-Volterra Communities". In: *Physics Review Letters* 130 (2023).

[36] Joseph W. Baron et al. "Non-Gaussian random matrices determine the stability of Lotka-Volterra communities". In: *arXiv preprint arXiv:2202.09140* (2022).